Ablation of PI3K p110-α Prevents High-Fat Diet–Induced Liver Steatosis

Mohar Chattopadhyay,[1] Elzbieta S. Selinger,[2] Lisa M. Ballou,[2] and Richard Z. Lin[1,2,3]

OBJECTIVE—To determine whether the phosphoinositide 3-kinase (PI3K) catalytic subunits p110-α and p110-β play a role in liver steatosis induced by a high-fat diet (HFD).

RESEARCH DESIGN AND METHODS—Liver-specific p110-α and p110-β knockout mice and control animals for each group were fed an HFD or normal chow for 8 weeks. Biochemical assays and quantitative real-time PCR were used to measure triglyceride, expression of lipogenic and gluconeogenic genes, and activity of protein kinases downstream of PI3K in liver lysates. Fatty acid uptake and incorporation into triglycerides were assessed in isolated hepatocytes.

RESULTS—Hepatic triglyceride levels in HFD-fed p110-$\alpha^{-/-}$ mice were 84 ± 3% lower than in p110-$\alpha^{+/+}$ mice, whereas the loss of p110-β did not significantly alter liver lipid accumulation. p110-$\alpha^{-/-}$ livers also showed a reduction in atypical protein kinase C activity and decreased mRNA and protein expression of several lipogenic genes. Hepatocytes isolated from p110-$\alpha^{-/-}$ mice exhibited decreased palmitate uptake and reduced fatty acid incorporation into triglycerides as compared with p110-$\alpha^{+/+}$ cells, and hepatic expression of liver fatty acid binding protein was lower in p110-$\alpha^{-/-}$ mice fed the HFD as compared with controls. Ablation of neither p110-α nor p110-β ameliorated glucose intolerance induced by the HFD, and genes involved in gluconeogenesis were upregulated in the liver of both knockout animals.

CONCLUSIONS—PI3K p110-α, and not p110-β, promotes liver steatosis in mice fed an HFD. p110-α might exert this effect in part through activation of atypical protein kinase C, upregulation of lipogenesis, and increased uptake of fatty acids. ***Diabetes*** **60: 1483–1492, 2011**

Nonalcoholic fatty liver disease (NAFLD) is one of the most common liver disorders worldwide and may affect up to one-third of adults in the U.S. (1,2). NAFLD is especially prevalent in people with type 2 diabetes, obesity, and/or hyperlipidemia. Simple steatosis in NAFLD may progress to steatohepatitis, advanced fibrosis, cirrhosis, and liver failure. Liver steatosis is characterized by the accumulation of excess triglycerides resulting from an imbalance between synthesis, uptake, secretion, and oxidation of fatty acids. It is well established that a high-fat diet (HFD) can induce hepatic steatosis in humans and rodents. HFDs can cause an increase in expression of the transcription factors sterol regulatory element binding protein 1c (SREBP-1c; a major activator of lipogenic genes) and peroxisome proliferator-activated receptor γ (PPAR-γ), and lipogenic genes such as fatty acid synthase (FAS) and acetyl-CoA carboxylase (ACC) in mouse liver (3,4). It would seem paradoxical to have increased lipogenesis in the face of excess dietary fats, and some studies have questioned whether HFD-induced liver steatosis is mainly a result of de novo lipogenesis (5). Another possible mechanism for high triglyceride accumulation in the liver could be increased uptake of dietary fatty acids from the blood. Fatty acid uptake in the liver is thought to be mediated by several transport proteins, including members of the fatty acid transport protein family and the highly expressed liver fatty acid binding protein (L-FABP). Deletion of these genes decreases fatty acid uptake in hepatocytes and partially protects mice from HFD-induced liver steatosis (6–9).

Class IA phosphoinositide 3-kinases (PI3Ks) are heterodimers consisting of a catalytic subunit (p110-α, p110-β, or p110-δ) bound to one of several regulatory subunits (collectively called p85). Analysis of the function of catalytic (p110-α and p110-β) and regulatory (p85-α and p85-β) subunits using knockout mice has shown that these enzymes regulate lipid and glucose metabolism in the liver under normal feeding conditions (10–12). Production of the second messenger phosphatidylinositol 3,4,5-trisphosphate by PI3Ks leads to activation of Akt and atypical protein kinase C (aPKC)-λ and -ζ (13–15). It has been proposed that Akt controls hepatic glucose metabolism downstream of PI3K in part by inhibiting expression of the major gluconeogenic genes phosphoenolpyruvate carboxykinase (*PEPCK*) and glucose 6-phosphatase (*G6PC*), whereas aPKC regulates lipid metabolism by upregulating the expression of SREBP-1c (12,16–18). However, two recent reports showed that liver steatosis in mice fed an HFD was improved in the absence of hepatic Akt2 (19) or upon inhibition of aPKC using adenoviral delivery of a kinase-dead enzyme (20), suggesting that both of these kinases can promote hepatic lipid accumulation under conditions of high dietary fat.

These results also suggest that PI3Ks are involved in HFD-induced liver steatosis. To test this hypothesis, we derived liver-specific p110-α– and p110-β–null animals from conditional PI3K knockout mouse strains previously generated by us (21). Using these animals, we show that ablation of p110-α, but not p110-β, attenuates liver steatosis induced by an HFD.

RESEARCH DESIGN AND METHODS

Materials. Antibodies were purchased from the following sources: for p110-α from BD Biosciences; for p110-β, p110-δ, Akt, aPKC (recognizes PKC-ζ and -λ), insulin receptor substrate-1 (IRS-1), IRS-2, Foxo1, SREBP-1, and S6 from

From the [1]Department of Physiology and Biophysics, Stony Brook University, Stony Brook, New York; the [2]Department of Medicine, Stony Brook University, Stony Brook, New York; and the [3]Department of Veterans Affairs Medical Center, Northport, New York.
Corresponding author: Richard Z. Lin, richard.lin@sunysb.edu.
Received 22 June 2010 and accepted 27 February 2011.
DOI: 10.2337/db10-0869
This article contains Supplementary Data online at http://diabetes.diabetesjournals.org/lookup/suppl/doi:10.2337/db10-0869/-/DC1.

Santa Cruz Biotechnology; for pan-p85 and glycogen synthase kinase 3β (GSK3β) from Millipore; for phospho-Akt, phospho-GSK3β (Ser 9), phospho-S6 (Ser 240/244), ACC (recognizes ACC1 and ACC2), phospho-Foxo1, and FAS from Cell Signaling; for L-FABP from Abcam; and for actin and glyceraldehyde 3-phosphate dehydrogenase (GAPDH) from Sigma-Aldrich.

Animals. *p110-α*$^{Flox/Flox}$ and *p110-β*$^{Flox/Flox}$ mice in a mixed 129 and C57BL/6 J genetic background (21) were bred to albumin-Cre (*Alb-Cre*) transgenic mice (Jackson Laboratory) to produce liver-specific p110-α and p110-β knockout mice. The one copy of *Alb-Cre* in both lines was detected by primers that span part of the *Cre* sequence. Only male mice were used in this study. *p110-α*$^{Flox/Flox}$;*Alb-Cre*$^{+}$ mice (referred to as p110-α$^{-/-}$) were compared with *p110-α*$^{Flox/Flox}$ (referred to as p110-α$^{+/+}$) littermates and *p110-β*$^{Flox/Flox}$;*Alb-Cre*$^{+}$ mice (referred to as p110-β$^{-/-}$) were compared with *p110-β*$^{Flox/Flox}$ (referred to as p110-β$^{+/+}$) littermates. Mice were analyzed between 8 and 16 weeks of age and were housed on a 12-h light/12-h dark cycle. For HFD experiments, 8-week-old mice were singly housed and fed either an HFD containing 45 kcal% fat (rodent diet D12451; Research Diets) or standard rodent chow for 8 weeks. Body weight and food intake were monitored weekly. Before the start and at the end of the study, mice were weighed and anesthetized and dual energy X-ray absorptiometry (DEXA) scanning was performed using the PIXImus2 DEXA scanner (Faxitron X-ray Corporation, Wheeling, IL) to determine body fat content. All animal-related experimental protocols were approved by the Stony Brook University Institutional Animal Care and Use Committee.

Western blotting. To determine tissue levels of PI3K, equal amounts of lysate protein were incubated for 2 h at 4°C with a phosphotyrosine peptide (CDMSKDESVDYpVPMLDMK) coupled to agarose (21). After four washes, the beads were boiled in SDS sample buffer and the proteins were subjected to Western blotting. For in vivo insulin signaling, mice were fasted overnight and then injected intraperitoneally with 2 units/kg body wt of human insulin (Novolin; Novo Nordisk) or an equal volume of saline. At different times after injection, mice were killed and livers were removed and frozen in liquid nitrogen. Liver extracts were subjected to SDS-PAGE and immunoblotting as previously described (22). Signals were visualized using horseradish peroxidase-linked secondary antibodies and chemiluminescence reagents.

Kinase assays. For PI3K assays, mice were fasted overnight, then anesthetized and injected through the inferior vena cava with insulin (2 units/kg). Livers were removed 5 min later and frozen in liquid nitrogen. Extracts were incubated overnight at 4°C with anti-IRS-1 or anti-IRS-2 antibody. Immunocomplexes were pulled down with protein A agarose and PI3K was assayed as previously described (22). For Akt and aPKC, mice on normal chow were fasted overnight and then injected intraperitoneally with insulin (2 units/kg) or an equal volume of saline. Livers were removed 15 min later and frozen in liquid nitrogen. For mice on the HFD, livers were removed from mice fasted for 6 h without any injections. Extracts were incubated overnight at 4°C with antibodies to Akt or aPKC. The immunoprecipitates were assayed as previously described (23).

Liver triglyceride content. Mice fasted for 6 h were killed, and tissues were frozen in liquid nitrogen. Frozen tissues (20–100 mg) were homogenized in PBS and extracted with chloroform and methanol (3:1). The extracts were dried overnight and resuspended in isopropanol. An appropriate volume of the suspension was assayed using a triglyceride assay kit (Sigma-Aldrich).

Hepatocyte isolation. Primary hepatocytes from mice fed normal chow were isolated by collagenase perfusion (24). Mice were anesthetized with ketamine/xylazine, and the liver was perfused first with Krebs Ringer buffer (122 mmol/L NaCl, 5.6 mmol/L KCl, 5.5 mmol/L D-glucose, 2.5 mmol/L $NaHCO_3$, and 20 mmol/L HEPES [pH 7.4]) with 0.1 mmol/L EGTA, followed by perfusion with Krebs Ringer buffer with 1.37 mmol/L $CaCl_2$ and 28 mg/50 mL collagenase (Worthington, type I). Both buffers were run at 5 mL/min for 10 min. Hepatocytes were harvested, and viability was examined by trypan blue exclusion. Hepatocytes were plated on collagen-coated plates in Dulbecco's modified Eagle's medium/F12-Ham's medium supplemented with 10% FBS, 1% antibiotic/antimycotic reagent (Sigma-Aldrich), 1 g/L fatty acid-free BSA, and 1× insulin-selenium-transferrin (Gibco). Cells were allowed to recover overnight before using them for experiments.

Long chain fatty acid uptake and incorporation into triglycerides. For fatty acid uptake, hepatocytes in PBS were incubated at 37°C for 30 min with or without 100 nmol/L insulin and then increasing concentrations of [^{3}H] palmitate bound to defatted BSA in a 3:1 molar ratio were added. After 1 min, uptake was stopped by adding 200 μmol/L phloretin/0.1% BSA at 4°C. The cells were washed three times with ice-cold PBS, lysed in 0.1 mol/L NaOH, 0.03% SDS, and protein content was measured (BCA assay; Thermo Scientific). Cellular uptake of [^{3}H]palmitate was determined by scintillation counting and normalized to total protein. [^{3}H]palmitate incorporation into triglycerides was performed as described previously with slight modifications (25). Hepatocytes were incubated for 2 h with or without 100 nmol/L insulin and with 0.04 mmol/L [^{3}H]palmitate bound to defatted BSA in a molar ratio of 3:1. Following treatment, cells were scraped off the plate in PBS and pelleted at 800 *g* at 4°C. The cells were extracted with 1 mL 2-propanol:heptane (4:1) for 1 h at room temperature with intermittent vortexing. After addition of 2 mL water and 2 mL heptane, the upper heptane phase containing triglyceride was collected and washed with ethanolic NaOH (ethanol:0.1 mol/L NaOH, 1:1). Triplicate samples of the washed heptane phase were dried in scintillation vials overnight. [^{3}H] palmitate incorporated into triglyceride was determined by scintillation counting and normalized to the number of cells plated.

Glucose tolerance test and blood chemistry. For glucose tolerance tests, mice fasted overnight were injected intraperitoneally with 2 g/kg dextrose and tail blood glucose was measured at various times using a One Touch Ultra Mini glucose monitor (Life Span, Milpitas, CA). Serum insulin levels were measured by ELISA (Crystal Chem, Chicago, IL). Serum levels of liver enzymes, bilirubin, cholesterol, triglyceride, albumin, and total protein were measured by Anilytics (Gaithersburg, MD).

Analysis of liver glycogen. Mice fasted for 6 h were killed, and livers were frozen in liquid nitrogen. Frozen livers (20–100 mg) were digested in 30% KOH for 20 min at 100°C. Macromolecules were precipitated by the addition of two volumes of ethanol followed by overnight incubation at −20°C. The next day the samples were centrifuged at 3,000 rpm for 15 min at 4°C and the supernatant was removed. Macromolecules were resuspended in water and precipitated again by addition of two volumes of ethanol and incubation overnight at −20°C. Macromolecules were washed in 70% ethanol, and glycogen was hydrolyzed by digestion in 84% H_2SO_4. Glucose in the samples was determined colorimetrically as compared with glucose standards after addition of anthrone.

Histology. Tissues were formalin fixed and embedded in paraffin using standard procedures. Sections (5 μm) were cut and stained with hematoxylin and eosin (H-E) or trichrome for standard microscopy. Frozen liver sections (8 μm) were stained with Oil Red O (Sigma-Aldrich) and counterstained with hematoxylin to visualize lipids.

Quantitative real-time (RT)-PCR. Quantitative RT-PCR was performed as described previously (26). Total RNA was extracted from livers using Tri Reagent (Sigma-Aldrich), and cDNA was generated using the iScript cDNA Synthesis kit (Bio-Rad). TaqMan Universal PCR Master Mix and TaqMan gene expression assays for Fasn (Mm00662312_g1), Srebf1 (Mm00550338_m1), Pparg (Mm01184323_m1), Fabp1 (Mm00444340_m1), Pck1 (Mm01247057_g1), G6pc (Mm00839363_m1), Acaca (Mm01304285_m1), and 18S RNA (HS99999901_s1) were purchased from Applied Biosystems. RT-PCR was performed on duplicate samples using a DNA Engine Opticon 2 System (MJ Research). The abundance of mRNA of the gene of interest relative to 18S RNA was determined using the equation $r = 2^{(C_{T\,18S\ RNA} - C_{T\,gene\ of\ interest})}$, where C_T is the number of cycles needed to achieve a preset threshold value of fluorescence. The results are expressed as fold change in r as compared with control samples.

Statistical analysis. Student *t* test was used for comparisons between groups using Excel Analysis Tool (Microsoft). Data are presented as mean ± SEM or % of control. $P < 0.05$ was considered to be significant.

RESULTS

Phenotypes of liver-specific p110-α and p110-β knockout mice. Hepatocyte-specific p110-α– and p110-β–deficient mice were generated as described in RESEARCH DESIGN AND METHODS. Western blotting confirmed that p110-α or p110-β was appropriately ablated (Fig. 1*A*) and that the gene deletion was specifically targeted to the liver (Fig. 1*B*). Both knockout mouse strains appeared normal and were fertile. At 9 weeks of age, there were no significant differences between control and knockout animals in body weight, liver protein content, or serum biochemical parameters that assess liver function (Table 1). However, the liver weight as a percentage of body weight and the liver triglyceride content of p110-α$^{-/-}$ mice were both significantly decreased as compared with p110-α$^{+/+}$ mice (Table 1). These values were not significantly different between p110-β$^{+/+}$ and p110-β$^{-/-}$ mice (Table 1). The liver glycogen content was reduced in both groups of knockout mice, and serum glucose and insulin were elevated in the p110-β$^{-/-}$ mice as compared with controls (Table 1). Gross examination of livers from 9-week-old mice revealed that the general lobular architecture of the organ was preserved in both knockout mouse strains.

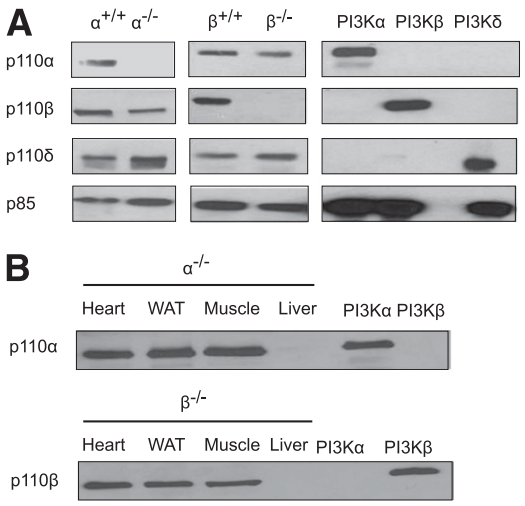

FIG. 1. Ablation of p110-α− and p110-β−PI3K in the liver. *A*: Class IA PI3Ks in liver lysates from mice of the indicated genotypes were pulled down with a phosphotyrosine peptide and the bound proteins were examined on Western blots probed with the indicated antibodies. Recombinant PI3K-α (p110-α/p85-α), PI3K-β (p110-β/p85-α), and PI3K-δ (p110-δ/p85-α) were loaded as controls. *B*: Class IA PI3Ks in lysates from hearts, white adipose tissue (WAT), skeletal muscle, and livers of p110-$\alpha^{-/-}$ and p110-$\beta^{-/-}$ mice were pulled down with a phosphotyrosine peptide, and the bound proteins were examined on Western blots probed with the indicated antibodies. Recombinant PI3K-α and PI3K-β were loaded as controls.

Histological analysis of liver sections revealed no obvious abnormalities such as necrosis or fibrosis (Supplementary Fig. 1).

Effect of PI3K ablation on hepatic insulin signaling. To investigate the effect of PI3K ablation on insulin signaling in the liver, mice were injected with insulin and Western blotting was used to assess the time course of Akt phosphorylation. Insulin-induced Akt phosphorylation at Ser473 was decreased in the p110-$\alpha^{-/-}$ and p110-$\beta^{-/-}$ livers, but phosphorylation at Thr308 was less affected (Fig. 2*A*). Insulin-stimulated phosphorylation of GSK3β and S6 was also rather indifferent to the loss of p110-$\alpha^{-/-}$ or p110-$\beta^{-/-}$ (Fig. 2*A*). We next assayed kinase activities in liver lysates of mice treated for 15 min with saline or hormone. Insulin activation of Akt was reduced by 49 ± 4% in the p110-$\alpha^{-/-}$ livers as compared with p110-$\alpha^{+/+}$ controls, whereas the activation of Akt was similar in the p110-$\beta^{-/-}$ and control livers (Fig. 2*B*). Because the residual Akt activation in p110-$\alpha^{-/-}$ liver appeared to be sufficient to increase the phosphorylation of GSK3β and S6 in response to insulin (Fig. 2*A*), we also examined Akt phosphorylation sites in the transcription factor Foxo1, which controls PEPCK expression (27). Insulin induction of Thr24 phosphorylation still occurred in p110-$\alpha^{-/-}$ liver, but the response at Ser319 was lost (Supplementary Fig. 2). Insulin-induced phosphorylation of Foxo1 at Ser256 was not observed in the liver of control or p110-$\alpha^{-/-}$ mice, although it was readily detected in HepG2 cells (data not shown). Activation of aPKC was completely blocked in the p110-$\alpha^{-/-}$ liver but unaffected in the p110-$\beta^{-/-}$ tissue (Fig. 2*C*).

Finally, PI3K activity in IRS-1 and IRS-2 immunoprecipitates of liver lysates prepared from insulin-injected mice was measured. There was a 52 ± 6% reduction in IRS-1–associated PI3K activity (Fig. 2*D*) and an 87 ± 10% reduction in IRS-2–associated PI3K activity (Supplementary Fig. 3) in the p110-$\alpha^{-/-}$ samples as compared with controls. IRS-1– and IRS-2–associated PI3K activity was not reduced in the p110-$\beta^{-/-}$ liver lysates as compared with p110-$\beta^{+/+}$ samples (Fig. 2*D* and Supplementary Fig. 3). To determine which PI3K isoform might be contributing to the residual PI3K activity in the p110-$\alpha^{-/-}$ liver, IRS-1 immunoprecipitates were assayed in the presence of PI3K inhibitors IC87114 (p110-δ selective), TGX-221 (p110-β selective), or PI-103 (broad spectrum). IC87114 caused a 77 ± 3% inhibition of PI3K activity in the p110-$\alpha^{-/-}$ immunoprecipitate and a 51 ± 3% decrease in the p110-$\alpha^{+/+}$ immunoprecipitate (Fig. 2*D*). Treatment with TGX-221 did not inhibit the PI3K activity in p110-$\alpha^{-/-}$ samples, whereas PI-103 inhibited the activity by 84 ± 3% (Fig. 2*D*). Western blot analysis of liver extracts detected p110-δ in the livers of all four strains of mice (Fig. 1*A*). These data show that insulin signaling through IRS-1 and IRS-2 to activate Akt and aPKC is mediated by p110-α but not p110-β. The

TABLE 1
Phenotypic comparison of p110 control and knockout mice on normal chow

	p110-$\alpha^{+/+}$	p110-$\alpha^{-/-}$	p110-$\beta^{+/+}$	p110-$\beta^{-/-}$
Body weight (g)	22 ± 2	22 ± 1.6	22 ± 0.8	22 ± 1.3
%Body fat	18.3 ± 0.2	18.6 ± 0.5	17.2 ± 0.2	16.9 ± 0.2
Liver as % of body weight	4.00 ± 0.01	3.00 ± 0.02*	4.00 ± 0.02	4.00 ± 0.03
Liver triglyceride (mg/g)†	5.7 ± 0.9	4.1 ± 0.2*	5.1 ± 0.7	5.0 ± 0.2
Liver protein (mg/g)	346 ± 53	288 ± 20	326 ± 23	312 ± 52
Liver glycogen (mg/g)†	14.2 ± 0.3	5.8 ± 0.1*	13 ± 0.3	1.3 ± 0.3*
Blood chemistry†				
ALT (units/L)	65 ± 19	44 ± 2	232 ± 21	156 ± 33
AST (units/L)	180 ± 44	215 ± 40	264 ± 67	271 ± 92
ALP (units/L)	85 ± 15	89 ± 10	85 ± 14	88 ± 2
Total bilirubin (mg/dL)	0.1 ± 0.02	0.3 ± 0.01	0.2 ± 0.01	0.2 ± 0.1
Cholesterol (mg/dL)	50 ± 9	39 ± 2	74 ± 10	64 ± 5
Triglyceride (mg/dL)	50 ± 4	41 ± 4	63 ± 12	59 ± 7
Albumin (g/dL)	2.3 ± 0.1	2.1 ± 0.2	2.7 ± 0.2	2.3 ± 0.3
Total protein (g/dL)	3.6 ± 0.3	3.3 ± 0.4	4.4 ± 0.4	3.9 ± 0.1
Glucose (mg/dL)	119 ± 2	118 ± 1	109 ± 4	150 ± 4*
Insulin (ng/mL)	1.96 ± 0.32	1.82 ± 0.21	0.75 ± 0.11	3.46 ± 0.53*

Data are means ± SE; $N = 6$ per group. ALT, alanine aminotransferase; AST, aspartate aminotransferase; ALP, alkaline phosphatase. *$P < 0.05$. †Animals were fasted for 6 h.

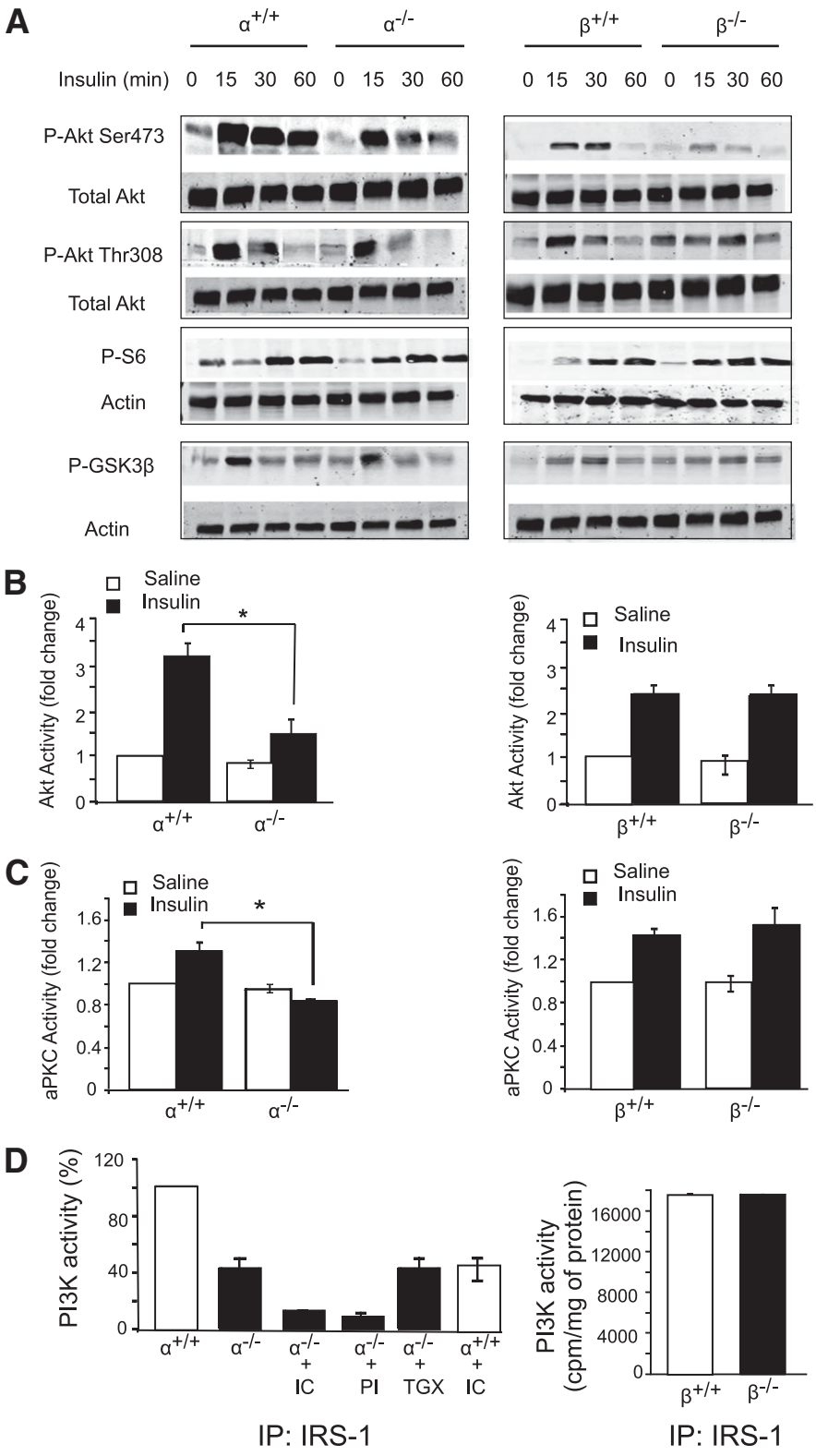

FIG. 2. Insulin signaling in p110-null livers. *A*: Liver lysates from fasted mice treated intraperitoneally without or with insulin (2 units/kg body wt) for the indicated times were analyzed by Western blotting. *B* and *C*: Fasted mice were injected intraperitoneally with saline or insulin (2 units/kg body wt). Livers were collected 15 min later, and lysates were prepared and assayed for Akt (*B*) or aPKC (*C*) kinase activity. *$P < 0.05$ by t test ($N = 3$ for all groups). *D*: Mice were fasted overnight and then injected through the inferior vena cava with insulin (2 units/kg body wt). Livers were collected 5 min later, and lysates were subjected to immunoprecipitation with IRS-1 antibody. The immunoprecipitates for p110-$\alpha^{+/+}$ and p110-$\alpha^{-/-}$ (*left panel*) were assayed for PI3K activity in the presence of vehicle, 500 nmol/L PI-103 (PI), 50 nmol/L TGX-221 (TGX), or 5 μmol/L IC87114 (IC). Values are normalized to the average PI3K activity in p110-$\alpha^{+/+}$ samples assayed in the absence of inhibitors. The immunoprecipitates for p110-$\beta^{+/+}$ and p110-$\beta^{-/-}$ (*right panel*) were assayed without any additions ($N = 3$ for all groups). Values shown are mean ± SEM.

results also suggest that a significant portion of insulin-activated PI3K activity in the liver is contributed by p110-δ.

Effect of PI3K ablation on HFD-induced liver steatosis. To investigate the role of PI3K isoforms in the development of HFD-induced liver steatosis, these four mouse strains were fed an HFD for 8 weeks. All four groups of mice gained weight (9.8 ± 0.2 g) and body fat (average increase of 42 ± 0.4% by DEXA scan). There were no significant differences in these parameters between p110-deficient animals and their $p110^{+/+}$ controls. All four strains of mice were hyperinsulinemic and hyperglycemic under HFD conditions (Table 2). There were no significant differences in serum triglyceride levels between the knockout and control animals on the HFD (Table 2). However, ablation of p110-α markedly reduced liver lipid accumulation as compared with controls as assessed by Oil Red O staining of liver sections (Fig. 3*A*). Hepatic triglyceride levels in HFD-fed p110-$\alpha^{-/-}$ mice were 84 ± 3% lower than in p110-$\alpha^{+/+}$ mice (Fig. 3*B*). In contrast, loss of p110-β did not significantly affect liver lipid accumulation in mice fed the HFD (Fig. 3*A* and *B*). aPKC and Akt activities were assayed in liver extracts of HFD-fed mice that were fasted for 6 h. aPKC activity was significantly decreased in the p110-$\alpha^{-/-}$ livers as compared with p110-$\alpha^{+/+}$ controls (Fig. 3*C*), but there was no significant difference in Akt activity between these two groups (Fig. 3*D*). In contrast, neither aPKC nor Akt was affected by ablation of p110-β (Fig. 3*C* and *D*). Thus reduced aPKC activity in p110-$\alpha^{-/-}$ livers correlates with their resistance to HFD-induced steatosis.

Ablation of p110-α decreases lipogenic gene expression. HFDs can upregulate the expression of lipogenic genes in livers of mice (3,4). Using quantitative RT-PCR, we found that under fed conditions the expression of FAS, PPAR-γ, SREBP-1, and ACC1 was upregulated in both p110-$\alpha^{+/+}$ and p110-$\alpha^{-/-}$ mice fed the HFD as compared with normal chow (Fig. 4*A*). However, with both diets the FAS, PPAR-γ, and SREBP-1 mRNA levels were significantly lower in p110-$\alpha^{-/-}$ livers than in p110-$\alpha^{+/+}$ livers (Fig. 4*A*). Western blotting showed that in mice fed normal chow, the SREBP-1 protein level was lower in p110-$\alpha^{-/-}$ livers than in p110-$\alpha^{+/+}$ livers (Fig. 4*B*). In mice fed the HFD, the hepatic FAS, ACC, and SREBP-1 protein levels were significantly reduced in p110-$\alpha^{-/-}$ as compared with p110-$\alpha^{+/+}$ mice (Fig. 4*B*). A similar analysis of livers from mice fasted for 6 h also showed increases in FAS, PPAR-γ, and SREBP-1 mRNAs in p110-$\alpha^{-/-}$ and p110-$\alpha^{+/+}$ mice fed the HFD as compared with normal chow (Fig. 4*C*). With both diets the FAS and PPAR-γ mRNA levels were significantly lower in p110-$\alpha^{-/-}$ livers than in control livers (Fig. 4*C*). Western blotting showed that in fasted mice on normal chow, the FAS protein level was lower in p110-$\alpha^{-/-}$ livers than in p110-$\alpha^{+/+}$ livers (Fig. 4*D*). By contrast, hepatic FAS protein levels after a 6-h fast were similar in HFD-fed p110-$\alpha^{-/-}$ and p110-$\alpha^{+/+}$ mice (Fig. 4*D*). Ablation of p110-β did not affect the expression of these genes in the livers of fasted mice on either diet (Supplementary Fig. 4). These results suggest that decreased lipogenesis contributes to the lower hepatic triglyceride content in p110-$\alpha^{-/-}$ mice fed normal chow (Table 1) and may be a major reason why liver triglyceride accumulation is attenuated in p110-$\alpha^{-/-}$ mice fed an HFD.

Ablation of p110-α reduces hepatic fatty acid uptake. Mice with defective hepatic uptake of long chain fatty acids are partially protected from liver steatosis when fed an HFD (6,8,9). To determine whether long chain fatty acid uptake is affected by loss of p110-α, [^{3}H]palmitate uptake was assayed in hepatocytes isolated from p110-$\alpha^{+/+}$ and p110-$\alpha^{-/-}$ mice. p110-α–null hepatocytes exhibited decreased [^{3}H]palmitate uptake as compared with p110-$\alpha^{+/+}$ cells at most of the fatty acid concentrations tested (Fig. 5*A*). In agreement with previously published data (28), insulin had little or no stimulatory effect on fatty acid uptake in hepatocytes of either genotype (Supplementary Fig. 5*A*). To determine whether lower fatty acid uptake could contribute to decreased steatosis in the p110-$\alpha^{-/-}$ mice, we measured [^{3}H]palmitate incorporation into triglycerides and found that this process was markedly reduced in p110-$\alpha^{-/-}$ hepatocytes as compared with control cells in the absence (Fig. 5*B*) or presence (Supplementary Fig. 5*B*) of insulin. We next examined the expression of L-FABP, which regulates fatty acid uptake, intracellular transport, and metabolism in the liver and promotes the development of liver steatosis in response to an HFD (9). Although L-FABP mRNA levels were higher in both p110-$\alpha^{+/+}$ and p110-$\alpha^{-/-}$ mice fed the HFD as compared with normal chow, the knockout livers showed lower expression than controls under both conditions (Fig. 5*C*). Livers from p110-$\alpha^{-/-}$ mice also contained decreased amounts of L-FABP protein as compared with controls, especially in HFD-fed mice (Fig. 5*D*). These results suggest that p110-$\alpha^{-/-}$ mice are protected from HFD-induced liver steatosis at least in part because of downregulation of L-FABP and reduced fatty acid uptake and incorporation into triglycerides.

Effect of PI3K ablation on HFD-induced glucose intolerance. In addition to hepatic steatosis, an HFD induces glucose intolerance in mice. Indeed, glucose tolerance tests showed that both p110-$\alpha^{+/+}$ and p110-$\beta^{+/+}$ mice developed this phenotype after 8 weeks on the HFD (Fig. 6*A* and *B*). Ablation of neither p110-α nor p110-β ameliorated HFD-induced glucose intolerance. In fact, p110-$\alpha^{-/-}$ mice exhibited more severe glucose intolerance than p110-$\alpha^{+/+}$ animals on the HFD (Fig. 6*A*). Similarly, HFD-induced increases in *PEPCK* gene expression were not inhibited by ablation of p110-α or p110-β (Supplementary Fig. 6). Interestingly, expression of G6PC was elevated in p110-$\alpha^{-/-}$ and

TABLE 2
Blood chemistry comparison of p110 control and knockout mice on HFD

	p110-$\alpha^{+/+}$	p110-$\alpha^{-/-}$	p110-$\beta^{+/+}$	p110-$\beta^{-/-}$
ALT (units/L)	42 ± 5	39 ± 9	51 ± 16	48 ± 8
AST (units/L)	360 ± 58	245 ± 67*	406 ± 131	366 ± 115
ALP (units/L)	62 ± 18	43 ± 8	86 ± 20	36 ± 5
Total bilirubin (mg/dL)	0.3 ± 0.15	0.2 ± 0.04	0.1 ± 0.04	0.1 ± 0.04
Cholesterol (mg/dL)	126 ± 19	83 ± 24	105 ± 14	134 ± 21
Triglyceride (mg/dL)	48 ± 11	41 ± 7	47 ± 16	46 ± 7
Albumin (g/dL)	2.3 ± 0.2	1.9 ± 0.2	2.6 ± 0.2	2.4 ± 0.2
Total protein (g/dL)	4.3 ± 0.3	3.3 ± 0.4	4.5 ± 0.4	4.3 ± 0.3
Glucose (mg/dL)	179 ± 31	208 ± 35	195 ± 14	186 ± 13
Insulin (ng/mL)	4.94 ± 0.92	5.42 ± 0.42	4.21 ± 2.50	5.46 ± 1.72

Data are means ± SE; $N = 3$ per group. ALT, alanine aminotransferase; AST, aspartate aminotransferase; ALP, alkaline phosphatase. *$P < 0.05$. Animals were fasted for 6 h.

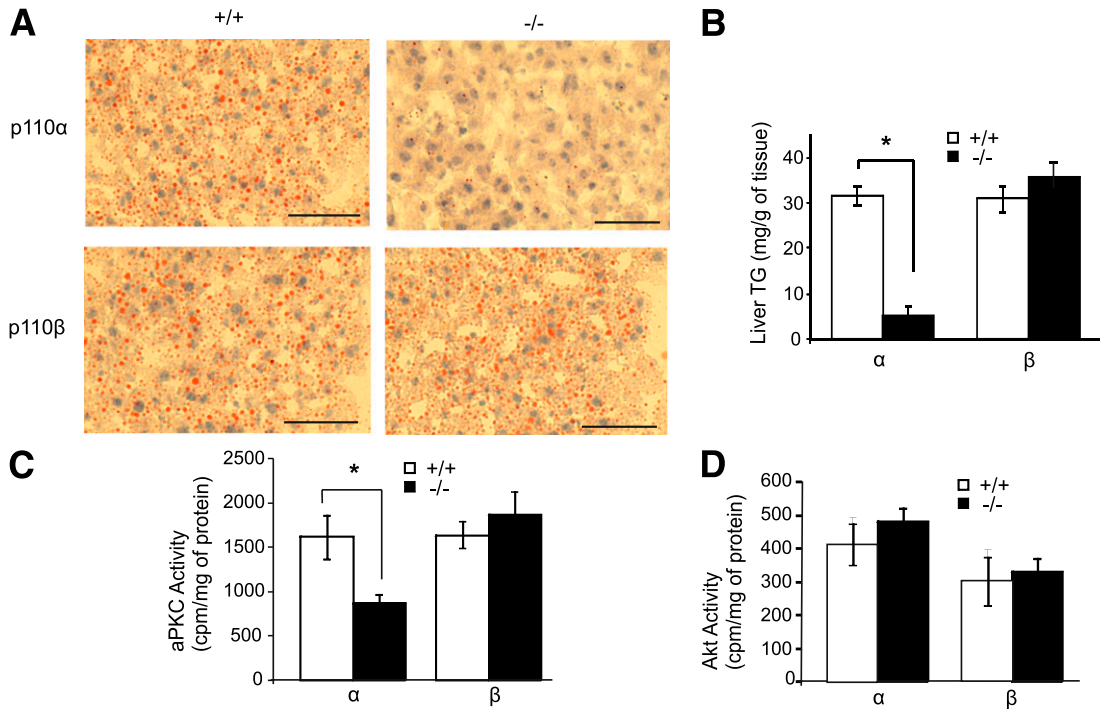

FIG. 3. Loss of p110-α blocks hepatic steatosis induced by an HFD. Mice were fed a 45 kcal% fat diet for 8 weeks. *A*: Frozen liver sections (8 μm) were stained with Oil Red O to visualize neutral lipids and counterstained with hematoxylin. Scale bars = 200 μm. *B*: Liver triglyceride (TG) content. *$P < 0.005$ by *t* test ($N = 6$). *C*: aPKC kinase activity assayed in liver lysates from mice fasted for 6 h. *$P < 0.01$ by *t* test ($N = 3$). *D*: Akt kinase activity assayed in liver lysates from mice fasted for 6 h ($N = 3$). Values are mean ± SEM. (A high-quality digital representation of this figure is available in the online issue.)

p110-$\beta^{-/-}$ animals fed normal chow as compared with their controls, but no further increase in G6PC mRNA was seen in the knockout livers of mice fed the HFD (Supplementary Fig. 6).

DISCUSSION

In this study, we found that HFD-induced hepatic steatosis was virtually eliminated in liver-specific p110-$\alpha^{-/-}$ mice, whereas ablation of p110-β had no effect on liver triglyceride accumulation. Recent studies have shown that inhibition of hepatic aPKC or Akt2 in mice ameliorates liver steatosis caused by an HFD (19,20). Indeed, the HFD-fed p110-$\alpha^{-/-}$ mice herein exhibited lower aPKC activity than the controls. A decrease in aPKC activity is thought to improve steatosis by reducing the expression of SREBP-1c and its lipogenic gene targets (20). Our finding that mRNA and/or protein levels of SREBP-1, FAS, PPAR-γ, and ACC were reduced in ab libitum–fed p110-$\alpha^{-/-}$ mice on the HFD is consistent with the idea that lipogenesis is reduced in the liver of these animals. Expression of some lipogenic genes was also suppressed in the liver of p110-$\alpha^{-/-}$ mice fed normal chow, as was the hepatic triglyceride content. These results suggest that p110-α ablation also inhibits lipid synthesis in the liver under normal dietary conditions.

Another source of triglycerides in the liver is uptake of fatty acids from the blood. It was estimated that about 74% of the triglyceride fatty acids in the liver of patients with NAFLD comes from serum nonesterified fatty acids plus dietary fatty acids (29). Several proteins have been identified that mediate fatty acid uptake into the liver, including L-FABP (30). In vitro studies demonstrated increased fatty acid uptake in cells with upregulated expression of L-FABP (31,32), and L-FABP knockout mice showed reduced fatty acid uptake in hepatocytes and decreased hepatic triglyceride when fed an HFD (8,9). We found that fatty acid uptake and incorporation into triglycerides were significantly decreased in p110-$\alpha^{-/-}$ hepatocytes. HFD caused an increase in L-FABP protein in control mice, but this increase was strongly inhibited in p110-$\alpha^{-/-}$ mice. Our results suggest that reduced fatty acid uptake as a consequence of decreased L-FABP expression is an important mechanism that protects p110-$\alpha^{-/-}$ mice from HFD-induced liver steatosis. Additional studies are needed to identify the mechanisms by which p110-α regulates L-FABP expression.

The hepatic insulin signaling pathways that suppress gluconeogenesis and activate lipogenesis have been proposed to bifurcate after Akt, with activation of mTORC1 (the rapamycin-sensitive complex of mammalian target of rapamycin) being required for insulin-stimulated induction of SREBP-1c but not for suppression of PEPCK (33). We found that expression of SREBP-1 was suppressed in the liver of p110-$\alpha^{-/-}$ mice on normal chow, but insulin activation of mTORC1 (as assessed by S6 phosphorylation) was intact. The apparent discrepancy in mTORC1 signaling and SREBP-1 expression between our work and that of Li et al. (33) could be because of differences between the two experimental systems, e.g., use of isolated rat hepatocytes treated with insulin for 6 h (33) versus mice injected with insulin for shorter times (this work). Another possibility is that the reduction in lipogenic gene expression in the p110-$\alpha^{-/-}$ liver occurs independently of insulin signaling. Elucidation of a possible role of p110-α in selective hepatic insulin signaling requires further study.

Previous studies using liver-specific p110-α– or p110-β–deficient mice examined the role of these PI3Ks in regulating glucose and lipid homeostasis under normal dietary conditions (10,11). Sopasakis et al. (11) examined chronic

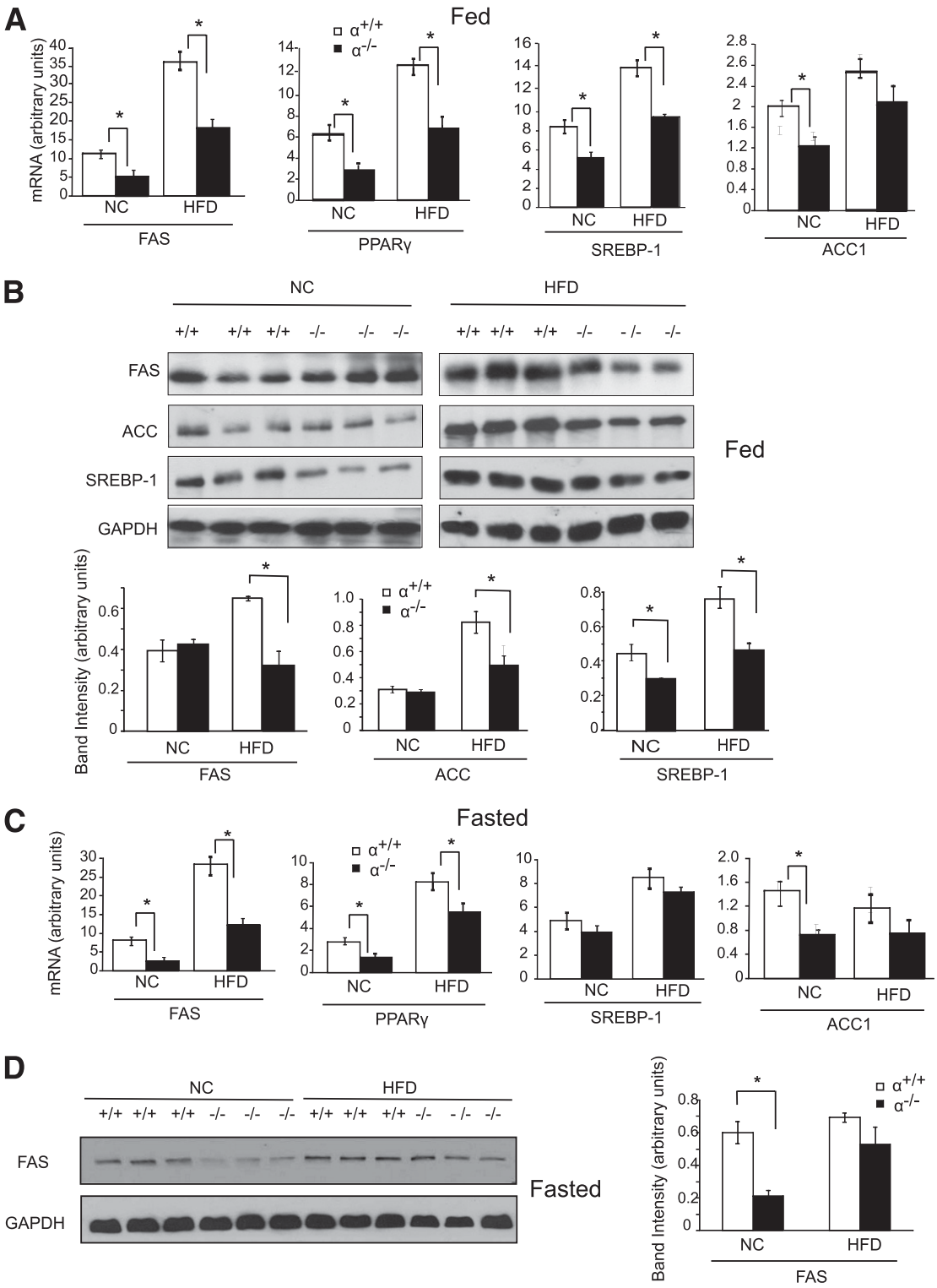

FIG. 4. Loss of p110-α affects the expression of genes and proteins regulating lipid metabolism. *A*: Quantitative RT-PCR analysis of mRNA levels in livers of mice fed ad libitum an HFD or normal chow (NC). *$P < 0.05$ by t test ($N = 6$). *B*: Liver lysates from ad libitum-fed mice were analyzed by Western blotting with the indicated antibodies. Bands were quantified using densitometry. *$P < 0.01$ by t test. *C*: Quantitative RT-PCR analysis of mRNA levels in livers of mice fasted for 6 h. *$P < 0.05$ by t test ($N = 6$). *D*: Liver lysates from mice fasted for 6 h were analyzed on Western blots, and the bands were quantified by densitometry. *$P < 0.01$ by t test. Values are means ± SEM.

(created by breeding a *p110-α*$^{Flox/Flox}$ line to *Alb-Cre* mice) and acute (created by injecting adult *p110-α*$^{Flox/Flox}$ mice with adenovirus expressing Cre) p110-α knockout mouse models. Both types of p110-α knockout mice exhibited reduced insulin sensitivity, impaired glucose tolerance, increased gluconeogenesis, hyperleptinemia, and hyperinsulinemia. There was almost a complete loss of insulin-induced IRS-1–associated PI3K activity and marked reduction in insulin activation of Akt and aPKC in the liver of chronic p110-α knockout mice (11). The acute p110-α knockout

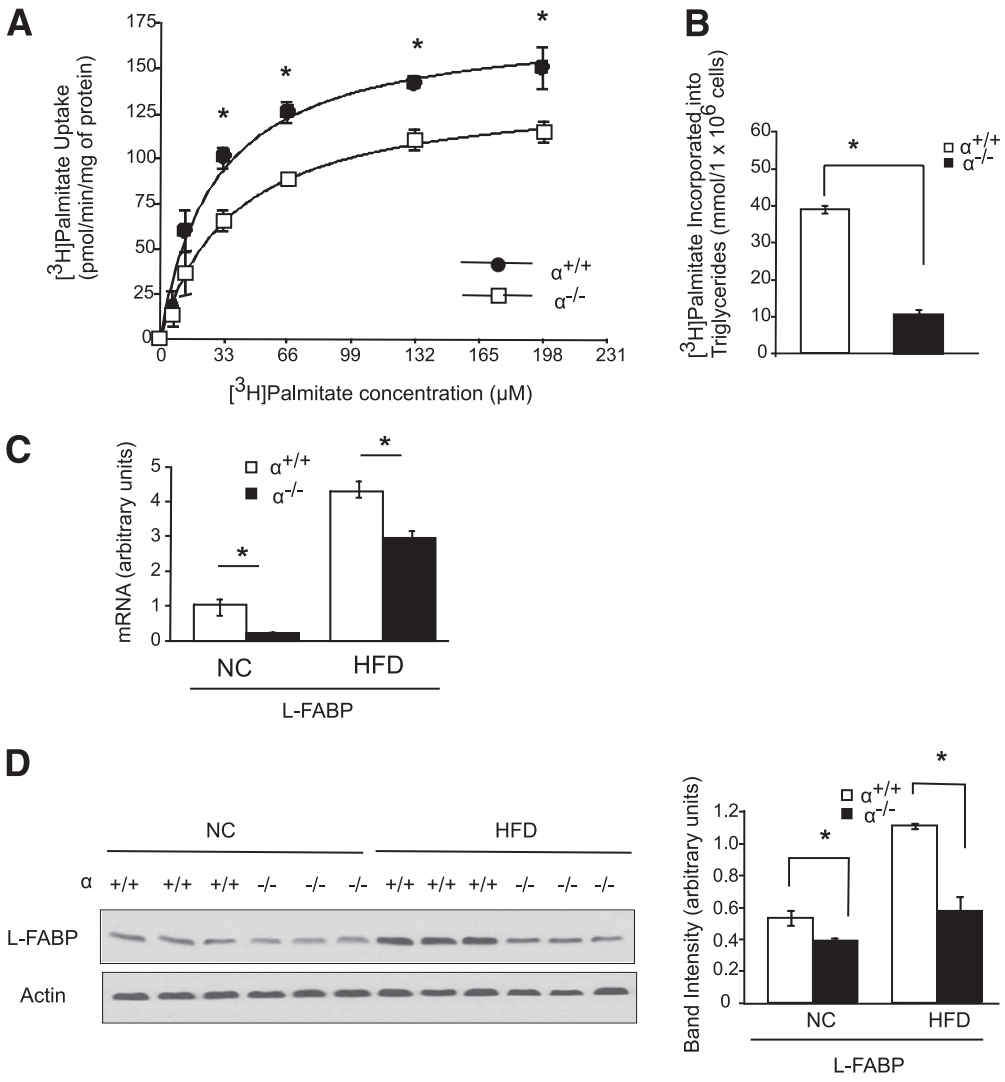

FIG. 5. Loss of p110-α attenuates fatty acid uptake in hepatocytes. Hepatocytes were isolated from p110-$\alpha^{+/+}$ and p110-$\alpha^{-/-}$ mice fed normal chow as described in RESEARCH DESIGN AND METHODS. *A*: Cells were incubated with increasing amounts of [^{3}H]palmitate/BSA at a 3:1 molar ratio for 1 min. [^{3}H]palmitate uptake into the cell was then measured. *$P < 0.001$ by *t* test. *B*: Hepatocytes were incubated with [^{3}H]palmitate/BSA for 2 h, and [^{3}H]palmitate incorporated into cellular triglycerides was then measured. *$P < 0.001$ by *t* test. *C*: Quantitative RT-PCR analysis of mRNA levels in livers of p110-$\alpha^{+/+}$ and p110-$\alpha^{-/-}$ mice fed an HFD or normal chow (NC). *$P < 0.05$ by *t* test ($N = 6$). *D*: Liver lysates were analyzed by Western blotting with the indicated antibodies. Bands were quantified using densitometry. *$P < 0.005$ by *t* test. Values are means ± SEM of three independent experiments done in triplicate.

mice (11) also exhibited decreases in liver triglyceride and expression of lipogenic genes, similar to our p110-$\alpha^{-/-}$ animals fed normal chow. The acute liver-specific p110-β knockout mice examined by Jia et al. (10) showed intact insulin activation of Akt in the liver, increased gluconeogenesis and hepatic PEPCK mRNA levels, hyperinsulinemia, hyperleptinemia, glucose intolerance, and reduced insulin sensitivity. Several of these phenotypes were also observed in our p110-$\beta^{-/-}$ mice on normal chow.

Activation of PI3K signaling controls many aspects of the insulin-mediated regulation of glucose metabolism. Insulin suppression of gluconeogenic genes is thought to be mediated by Akt-dependent phosphorylation and inhibition of Foxo1 (27). It was surprising that p110-$\beta^{-/-}$ mice on normal chow were hyperglycemic with increased expression of hepatic PEPCK and G6PC, since insulin activation of Akt appeared normal in these animals. This result suggests that an Akt-independent mechanism controls PEPCK expression in the p110-$\beta^{-/-}$ liver. Although insulin activation of PI3K and Akt were both attenuated in the liver of our p110-$\alpha^{-/-}$ mice fed normal chow, these effects did not lead to hyperglycemia. We suspect that the normal glucose levels in our p110-$\alpha^{-/-}$ mice fed normal chow are because of residual Akt activation in the liver, which is adequate to signal downstream. Indeed, insulin-stimulated phosphorylation of GSK3β, S6, and Thr24 in Foxo1 was unaffected in the p110-$\alpha^{-/-}$ liver, although phosphorylation of Ser319 in Foxo1 was suppressed. The residual Akt activation might be a result of recruitment of p110-δ into the IRS-1 complex following insulin stimulation. The p110-$\alpha^{-/-}$ mice used here may have a compensatory upregulation of p110-δ. However, we found that about 50% of the insulin-induced IRS-1–associated PI3K activity from control p110-$\alpha^{+/+}$ livers is contributed by p110-δ, based on its sensitivity to IC87114. It is possible that variable amounts of p110-δ in insulin-responsive tissues in different strains of mice could affect insulin action and the phenotypes of p110-α knockout animals. The

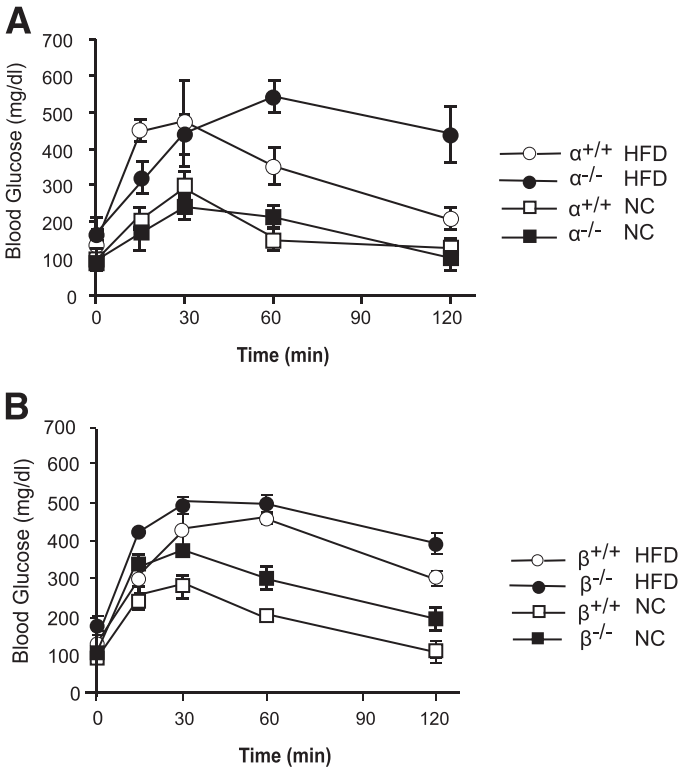

FIG. 6. Glucose intolerance in mice fed an HFD. *A* and *B*: Glucose tolerance tests in mice of the indicated genotypes fed an HFD or normal chow (NC) (*N* = 6 in each group).

hepatic level of p110-δ in knockout mouse strains used in Ref. 11 was not reported. Future studies using p110-δ knockout mice will help clarify the role of this PI3K isoform in regulating hepatic metabolic processes.

The degree of glucose intolerance was more severe in our p110-$\alpha^{-/-}$ mice as compared with controls when they were fed the HFD. Lipotoxicity caused by fatty acid metabolites such as diacylglycerol or ceramide is thought to be central to the pathogenesis of hepatic insulin resistance (34). Hepatic steatosis is generally accompanied by fasting hyperglycemia and glucose intolerance, but a disconnect between liver steatosis and hepatic insulin resistance has been observed in some mouse models. For example, mice overexpressing acyl-CoA:diacylglycerol acyltransferase 1 or 2 in the liver developed hepatic steatosis with increased amounts of putative lipotoxic intermediates, but they did not develop hepatic insulin resistance or hyperglycemia (35). Similar to our p110-$\alpha^{-/-}$ mice on the HFD, ablation of hepatic Akt2 in the *ob/ob* background reduced liver steatosis but did not improve hyperglycemia (19). One explanation for our result is that a lipotoxic metabolite that causes hepatic insulin resistance is still produced in the livers of p110-$\alpha^{-/-}$ mice on the HFD, despite the overall reduction in hepatic lipid. Alternatively, reduced insulin signaling through p110-α might be part of the mechanism that leads to the HFD-induced increase in hepatic glucose production, so genetic ablation of this enzyme would worsen this condition. Altered lipid metabolism in the liver might also promote hormonal and metabolic changes in extrahepatic tissues that contribute to HFD-induced hyperglycemia and glucose intolerance in p110-$\alpha^{-/-}$ animals. Even though glucose intolerance was not improved in p110-$\alpha^{-/-}$ mice, reversing steatosis might be beneficial because it would block the progression to more serious liver disease.

In conclusion, our data indicate that p110-α but not p110-β plays a pivotal role in the development of liver steatosis induced by HFD feeding. The mechanism of reduced lipid accumulation in the p110-$\alpha^{-/-}$ liver is likely the result of decreased lipogenesis because of suppression of lipogenic genes and lower fatty acid uptake resulting from decreased expression of L-FABP. Because NAFLD is becoming a public health problem of epidemic proportions, a better understanding of the pathways that regulate lipid accumulation in the liver is crucial for developing effective therapies for this important medical condition.

ACKNOWLEDGMENTS

This study was funded in part by grants from the American Diabetes Association, the Department of Veterans Affairs Merit Review Program, and the National Institutes of Health (DK-62722 and CA-136754).

No potential conflicts of interest relevant to this article were reported.

M.C. contributed to research data and wrote the manuscript. E.S.S. contributed to research data. L.M.B. and R.Z.L. contributed to designing the study, discussion, and manuscript editing.

Parts of this study were presented in abstract form at Keystone Symposia: PI 3-Kinase Signaling in Disease, Olympic Valley, California, 22–27 April 2009.

The authors thank Drs. Yongjun Fan (Stony Brook University) and Wei-Xing Zong (Stony Brook University) for helping them with the long chain fatty acid uptake assay.

REFERENCES

1. Angulo P. Nonalcoholic fatty liver disease. N Engl J Med 2002;346:1221–1231
2. Angulo P. GI epidemiology: nonalcoholic fatty liver disease. Aliment Pharmacol Ther 2007;25:883–889
3. Inoue M, Ohtake T, Motomura W, et al. Increased expression of PPARgamma in high fat diet-induced liver steatosis in mice. Biochem Biophys Res Commun 2005;336:215–222
4. Lin J, Yang R, Tarr PT, et al. Hyperlipidemic effects of dietary saturated fats mediated through PGC-1beta coactivation of SREBP. Cell 2005;120:261–273
5. Oosterveer MH, van Dijk TH, Tietge UJ, et al. High fat feeding induces hepatic fatty acid elongation in mice. PLoS ONE 2009;4:e6066
6. Doege H, Baillie RA, Ortegon AM, et al. Targeted deletion of FATP5 reveals multiple functions in liver metabolism: alterations in hepatic lipid homeostasis. Gastroenterology 2006;130:1245–1258
7. Falcon A, Doege H, Fluitt A, et al. FATP2 is a hepatic fatty acid transporter and peroxisomal very long-chain acyl-CoA synthetase. Am J Physiol Endocrinol Metab 2010;299:384–393
8. Newberry EP, Xie Y, Kennedy S, et al. Decreased hepatic triglyceride accumulation and altered fatty acid uptake in mice with deletion of the liver fatty acid-binding protein gene. J Biol Chem 2003;278:51664–51672
9. Newberry EP, Xie Y, Kennedy SM, Luo J, Davidson NO. Protection against Western diet-induced obesity and hepatic steatosis in liver fatty acid-binding protein knockout mice. Hepatology 2006;44:1191–1205
10. Jia S, Liu Z, Zhang S, et al. Essential roles of PI(3)K-p110beta in cell growth, metabolism and tumorigenesis. Nature 2008;454:776–779
11. Sopasakis VR, Liu P, Suzuki R, et al. Specific roles of the p110alpha isoform of phosphatidylinsositol 3-kinase in hepatic insulin signaling and metabolic regulation. Cell Metab 2010;11:220–230
12. Taniguchi CM, Kondo T, Sajan M, et al. Divergent regulation of hepatic glucose and lipid metabolism by phosphoinositide 3-kinase via Akt and PKClambda/zeta. Cell Metab 2006;3:343–353
13. Akimoto K, Takahashi R, Moriya S, et al. EGF or PDGF receptors activate atypical PKClambda through phosphatidylinositol 3-kinase. EMBO J 1996;15:788–798
14. Burgering BM, Coffer PJ. Protein kinase B (c-Akt) in phosphatidylinositol-3-OH kinase signal transduction. Nature 1995;376:599–602

15. Standaert ML, Galloway L, Karnam P, Bandyopadhyay G, Moscat J, Farese RV. Protein kinase C-zeta as a downstream effector of phosphatidylinositol 3-kinase during insulin stimulation in rat adipocytes. Potential role in glucose transport. J Biol Chem 1997;272:30075–30082
16. Li X, Monks B, Ge Q, Birnbaum MJ. Akt/PKB regulates hepatic metabolism by directly inhibiting PGC-1alpha transcription coactivator. Nature 2007; 447:1012–1016
17. Matsumoto M, Ogawa W, Akimoto K, et al. PKClambda in liver mediates insulin-induced SREBP-1c expression and determines both hepatic lipid content and overall insulin sensitivity. J Clin Invest 2003;112:935–944
18. Puigserver P, Rhee J, Donovan J, et al. Insulin-regulated hepatic gluconeogenesis through FOXO1-PGC-1alpha interaction. Nature 2003;423:550–555
19. Leavens KF, Easton RM, Shulman GI, Previs SF, Birnbaum MJ. Akt2 is required for hepatic lipid accumulation in models of insulin resistance. Cell Metab 2009;10:405–418
20. Sajan MP, Standaert ML, Nimal S, et al. The critical role of atypical protein kinase C in activating hepatic SREBP-1c and NFkappaB in obesity. J Lipid Res 2009;50:1133–1145
21. Lu Z, Jiang YP, Wang W, et al. Loss of cardiac phosphoinositide 3-kinase p110 alpha results in contractile dysfunction. Circulation 2009;120:318–325
22. Ballou LM, Cross ME, Huang S, McReynolds EM, Zhang BX, Lin RZ. Differential regulation of the phosphatidylinositol 3-kinase/Akt and p70 S6 kinase pathways by the alpha(1A)-adrenergic receptor in rat-1 fibroblasts. J Biol Chem 2000;275:4803–4809
23. Ballou LM, Tian PY, Lin HY, Jiang YP, Lin RZ. Dual regulation of glycogen synthase kinase-3beta by the alpha1A-adrenergic receptor. J Biol Chem 2001;276:40910–40916
24. Seglen PO. Preparation of isolated rat liver cells. Methods Cell Biol 1976; 13:29–83
25. Waterfield CJ, Asker DS, Timbrell JA. Triglyceride disposition in isolated hepatocytes after treatment with hydrazine. Chem Biol Interact 1997;107: 157–172
26. Fan G, Jiang YP, Lu Z, et al. A transgenic mouse model of heart failure using inducible Galpha q. J Biol Chem 2005;280:40337–40346
27. Barthel A, Schmoll D, Unterman TG. FoxO proteins in insulin action and metabolism. Trends Endocrinol Metab 2005;16:183–189
28. Wu Q, Ortegon AM, Tsang B, Doege H, Feingold KR, Stahl A. FATP1 is an insulin-sensitive fatty acid transporter involved in diet-induced obesity. Mol Cell Biol 2006;26:3455–3467
29. Donnelly KL, Smith CI, Schwarzenberg SJ, Jessurun J, Boldt MD, Parks EJ. Sources of fatty acids stored in liver and secreted via lipoproteins in patients with nonalcoholic fatty liver disease. J Clin Invest 2005;115:1343–1351
30. Atshaves BP, Martin GG, Hostetler HA, McIntosh AL, Kier AB, Schroeder F. Liver fatty acid-binding protein and obesity. J Nutr Biochem 2010;21: 1015–1032
31. Luxon BA, Milliano MT, Weisiger RA. Induction of hepatic cytosolic fatty acid binding protein with clofibrate accelerates both membrane and cytoplasmic transport of palmitate. Biochim Biophys Acta 2000;1487:309–318
32. Murphy EJ, Prows DR, Jefferson JR, Schroeder F. Liver fatty acid-binding protein expression in transfected fibroblasts stimulates fatty acid uptake and metabolism. Biochim Biophys Acta 1996;1301:191–198
33. Li S, Brown MS, Goldstein JL. Bifurcation of insulin signaling pathway in rat liver: mTORC1 required for stimulation of lipogenesis, but not inhibition of gluconeogenesis. Proc Natl Acad Sci USA 2010;107:3441–3446
34. Chavez JA, Summers SA. Lipid oversupply, selective insulin resistance, and lipotoxicity: molecular mechanisms. Biochim Biophys Acta 2010;1801: 252–265
35. Monetti M, Levin MC, Watt MJ, et al. Dissociation of hepatic steatosis and insulin resistance in mice overexpressing DGAT in the liver. Cell Metab 2007;6:69–78